

A DIACHRONIC ANALYSIS OF THE VEGETATION COVER IN A SPATE IRRIGATION PERIMETER – CASE STUDY: THE EL FEIDH REGION, BISKRA, ALGERIA

SALAH EDDINE MALLEM^{*1}, HAFIZA TATAR^{**}, MERIEM BOULTIF^{***}

Key-words: spate irrigation, remote sensing, El Feidh, NDVI, NDWI, SI, BI.

Abstract. This article aims to study a model of traditional agriculture using spate irrigation. To this end, we relied on a methodological approach based on the calculation of spectral indices: Normalized Difference Vegetation Index (NDVI), Normalized Difference Water Index (NDWI), Bare soil Index (BI), and Salinity Index (SI), which allowed us to evaluate the diachronic changes in the soil surface condition in the study area, particularly the evolution of the vegetation cover. The processing of multi-date Landsat images [1985–2020] revealed a widespread degradation in the vegetation cover at the El Feidh perimeter, as well as an increase in salinity. The results obtained indicate that in 1985, the average of the vegetation index (NDVI) was 0.49, which is very important compared to the years 2000 and 2020, when the average NDVI was 0.20 and 0.12, respectively. The vegetation cover area decreased from 98.89% in 1985 to 97.72% in 2000, only to drop again to 42.98% in 2020. In contrast, the average salinity index has increased over the years: it was lower in 1985 (SI = 952.04) than in 2020 (SI = 2261.63). Furthermore, the diachronic analysis of the NDWI shows that soil and plant moisture have also decreased significantly: the average NDWI was 0.19 in 1985, then dropped to -0.03 in 2000, only to drop again to -0.08 in 2020.

1. INTRODUCTION

As competition for water intensifies and commitments towards sustainable ecosystems are more frequent, there has been a growing awareness for the need to better use water, which is a rare and precious resource for all economic activities in water-scarce regions, such as Africa (Haouari & Azaiez, 2001; van Halsema; Vincent, 2012 & Athamena *et al.*, 2023). Irrigated agriculture, which accounts for approximately 40% of global production, consumes around 70% of the total fresh water available in the world (Salmon *et al.*, 2015; Ghebreamlak *et al.*, 2018).

In several regions of the world, irrigation techniques can be crucial to agricultural productivity in meeting the projected food demand because they can sustain or even increase crop yields in the face of shifting meteorological circumstances. Therefore, precise data on the amount, distribution, and variability of water usage in irrigated agriculture are crucial for evaluating water resources and agricultural output (Alexandridis *et al.*, 2014). One type of information that requires an accurate estimate is the irrigation system area (Brookfield *et al.*, 2024). It is an important input parameter for many irrigation performance indicators, such as water use, water productivity, water rights, water valuation,

* PhD Student, Laboratoire des Sciences du Territoire, Ressources Naturelles et Environnement (LASTERNE), University of Constantine 1 (Frères Mentouri University), Constantine, Algeria; Researcher, Scientific and Technical Research Center on Arid Regions (CRSTRA), Biskra, Algeria, salaheddine.ma.7@gmail.com.

** Professor, Laboratoire des Sciences du Territoire, Ressources Naturelles et Environnement (LASTERNE), University of Constantine 1 (Frères Mentouri University), Constantine, Algeria, hafizatatar@gmail.com.

*** Researcher, Scientific and Technical Research Center on Arid Regions (CRSTRA), Biskra, Algeria, bouldif.meriem05@gmail.com.

¹ Corresponding Author

impact, and performance diagnosis (Bastiaanssen *et al.*, 2000). Irrigation system data, including irrigated/cultivated areas, are rarely measured frequently and accurately to cover a complete irrigation system, despite their relevance in assessing irrigation performance indicators. According to Ambast *et al.* (2002), the conventional approach of gathering data through field observations is challenging, time-consuming, and insufficient in terms of temporal and spatial coverage. This leads to a lack of proper and effective management of the irrigation systems.

Remote sensing is an effective tool for mapping and monitoring irrigated crops owing to the synoptic nature of satellite data (Lamhamedi *et al.*, 2017; Koull *et al.*, 2022). Thanks to advances in satellite technology in terms of spatial, spectral, temporal, and radiometric resolutions, it is now possible to collect agricultural data at frequent intervals over a vast area (Bastiaanssen & Bos, 1999; Atzberger, 2013; Mondal *et al.*, 2014; Ghebreamlak *et al.*, 2018). Satellite observations provide reliable, economical, and synoptic data on the Earth's surface. In addition, they have made it possible to provide precise information on the types of crops (Dadhwal *et al.*, 2002; Schmedtmann & Campagnolo, 2015), yield (Bastiaanssen & Ali, 2003; Lobell, 2013), or evapotranspiration (Singh *et al.*, 2012; Liou & Kar, 2014). In addition, remote sensing techniques have become a viable option and are commonly used to map irrigated and cultivated areas (Biggs *et al.*, 2006; Alexandridis *et al.*, 2008; Pervez & Brown, 2010; Gumma *et al.*, 2011; Gallego *et al.*, 2014; Pervez *et al.*, 2014).

Moreover, rainwater collection and storage systems are widely recognized for their effectiveness (Freni & Liuzzo, 2019). Rainwater harvesting can supplement water resources and reduce pressure on groundwater reservoirs, especially in arid climates (Zuhriddin & Young-Jin, 2023). In addition, spate irrigation or directed flooding (sometimes called *floodwater harvesting*) is a form of random irrigation where farmers use floodwater from a dry river (*oued*). According to the FAO (2005), these irrigation systems usually have a vast catchment area upstream, ranging in area between 200 ha and 50 km². They also stand out through a significant ratio (collection area/cultivated area), ranging from 1/100 to 1/10,000.

Flood irrigation is a common practice in many parts of the world, notably in West Asia, Central Asia, the Near East, North Africa, the Horn of Africa, and Latin America, where Pakistan is the largest country subject to this type of irrigation. Unfortunately, in some regions, such as North Africa, this practice has been considerably reduced in recent decades due to the construction of dams on ephemeral rivers. By contrast, the Horn of Africa is experiencing a rapid increase in the area under flood irrigation, particularly in Ethiopia and Eritrea. This growth is largely due to demographic pressure and the settlement of populations on vast plains that are becoming increasingly habitable (FAO, 2010).

Regarding Algeria, because spate irrigation systems are still essential to agriculture in the country, the government places a high value on them. The government attaches high importance to flood irrigation systems because agriculture (particularly in the south of the country) still depends on them. Statistics concerning irrigation in Algeria indicate that part of the P.M.H.², notably the palm trees of the oases in the south, and seasonal crops such as grains (barley and wheat) in the Al-Dhyat (*oueds*) are irrigated using flood spreading. According to the FAO, the agricultural area covered by flood spreading is estimated at around 110,000 ha in 1984 (FAO, 1995), 56,050 ha in 2001 (FAO, 2005), and 53,000 ha in 2008 (FAO, 2015a).

In this study area, the only water resource which can irrigate the perimeter of El Feidh is the occurrence of various flood events from Oued El Arab. The difficulty lies in using these waters, which are as massive as they are unpredictable and ephemeral. The populations did not try to block this *oued* (which would have been beyond their technical capabilities) but used the natural tendency of the waters to spread over the slopes, amplifying the phenomenon, operating a rudimentary system of diversions.

² Small and medium hydraulics (in French: **Petite et Moyenne Hydraulique**).

Thus, they cause temporary submersion. On this “*maader*”³, such episodic irrigation cannot irrigate either gardens or palm trees; they are adequate only for grains (barley and wheat) (Côte, 2008).

Among the previous studies conducted on mapping spate irrigation zones, the research performed by Soomro *et al.* (2020) is worth mentioning. This study analysed the spatio-temporal variability of spate irrigation systems using remote sensing and GIS in Kirthar National Range, part of Pakistan’s Sindh province. The supervised maximum likelihood classification procedure, supplemented with secondary data, revealed a significant increase of 83.85% in spate irrigation systems during the period (2013–2018).

There is also a study by Ghebreamlak *et al.* (2018), where the authors used satellite remote sensing data to develop a methodology for mapping and estimating seasonally cultivated areas in the Gash Delta spate irrigation system. Visual interpretations followed by NDVI and a surface temperature (Ts) analysis were carried out on selected images during the cropping period, with a view to developing a threshold-based classification algorithm. The result of this study indicates that the comparison of the extracted cultivated area with the field report area showed a promising application of the methodology for mapping and estimating cultivated areas from remote sensing data alone.

Nevertheless, monitoring the changes in vegetation cover through spectral indices, in areas where infrastructure works have been installed, has been the subject of several studies. For example, Bid (2016) carried out a study on changes in vegetation cover in the watershed of the Panchet Hill dam (India), emphasizing that the construction of the Panchet Hill Dam in 1959 had to prevent the natural flow of the Damodar River, which affected the vegetation in the upper and lower parts of the watershed. The main objective of the study by Bid (2016) was to identify the change in vegetation patterns and the loss of green cover in the area using the NDVI technique. The results of this study showed that the change in total vegetation cover between 1990 and 2014 was negative, equivalent to –70.13%.

This study was motivated by a lack of research on spate irrigation perimeters and their spatial distribution in Algeria. The objectives of this study were to present the effectiveness of using remote sensing and GIS to monitor the evolution of land cover in a spate irrigation perimeter in the El Feidh region and to develop maps of the evolution of the NDVI, NDWI, BI, and SI spectral indices of this perimeter during the period (1985–2020).

2. MATERIALS AND METHODS

2.1. Study area

The perimeter of El Feidh extends mainly over the eastern region of the Wilaya of Biskra (Algeria). It belongs to the commune of El Feidh and spans an area of 60.376 km². The perimeter of El Feidh is situated between 34°23'8" and 34°31'17" latitude N and 6°28'57" and 6°35'41" longitude E (Fig. 1), with an elevation range between -51 m and 9 m. This perimeter belongs to the mild arid bioclimatic stage (Côte, 1998) with an average annual temperature of 22.36°C (1977–2013) and annual precipitation of 117.88 mm (1971–2013).

The Oued El Arab watershed (Fig. 1), spanning over 2,085 km², is located in the North-East of the large hydrographic basin of Chott Melrhir. The Oued El Arab results from the confluence of the Oued El Abiod⁴ and the Oued Mellagou, which respectively originate from the Djebel Aïdel and the Djebel Chélia.

The Oued El Arab records a flow of 0.71 m³/s on its route towards Chott Melrhir, at the Khangat Sidi Nadji hydrometric station⁵, located at the end of a 2,085 km² watershed (Mebariki, 2005). The mean

³ Area of spreading of runoff water, cultivation on spreading, silty plain likely to be irrigated during heavy rains.

⁴ Do not mistake this *oued* for Oued El Abiod, which flows through the commune of Arris.

⁵ The data relates to the period: 1972/73–1993/94.

annual discharge from the Oued El Arab watershed for the 1972–1994 period is 22.4 hm³/year. The hydrological yield of this watershed is relatively modest, with a specific flow rate of 0.34 l/s/km² (Mebarki, 2005).

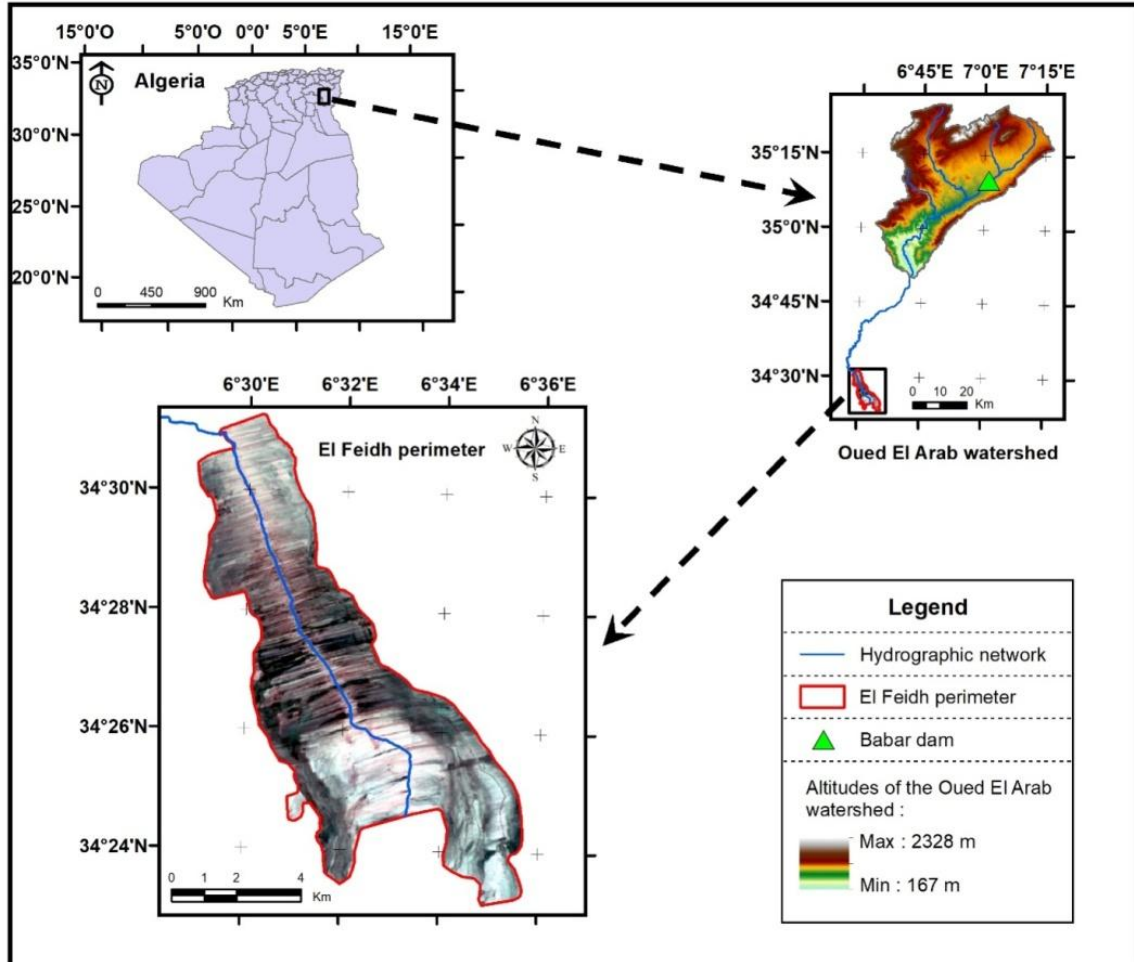


Fig. 1 – Location map of the study area.

2.2. Data collection

The images used consist of six scenes captured by the TM sensor on the Landsat 5 satellite. The images were acquired in 1985, 1990, 1995, 2000, 2005, and 2010, respectively, and two scenes from Landsat 8 satellite OLI-TIRS sensors were obtained in 2015 and 2020. These multispectral images, with a spatial resolution of 30 m, were processed using two software programs: ENVI (version 5.3) and ArcMap (version 10.2.2).

The Landsat image dataset used in this study is freely available on the USGS website. Downloading satellite images for this study is based on two criteria: crop interval (between February

and May, as it is the best period when the perimeter plants are well developed⁶) and cloud cover (satellite images containing clouds are avoided).

Table 1

Technical characteristics of the Landsat images used

Satellite	Sensor	Path/Row	Number of bands	Spatial resolution	Acquisition date
Landsat 5	TM (1 on-board sensor)	193/36	07	30 m (except: B6 = 120 m)	02 – 02 – 1985
		193/36	07	30 m (except: B6 = 120 m)	16 – 02 – 1990
		193/36	07	30 m (except: B6 = 120 m)	03 – 04 – 1995
		193/36	07	30 m (except: B6 = 120 m)	16 – 04 – 2000
		193/36	07	30 m (except: B6 = 120 m)	30 – 04 – 2005
		193/36	07	30 m (except: B6 = 120 m)	12 – 04 – 2010
Landsat 8	OLI-TIRS (2 on-board sensors)	193/36	11	30 m (except: B8 = 15 m B10 = 100 m B11 = 100 m)	12 – 05 – 2015
		193/36	11	30 m (except: B8 = 15 m B10 = 100 m B11 = 100 m)	07 – 04 – 2020

2.3. Methodology

To study the spatio-temporal evolution of the plant cover of the spate irrigation perimeter in the El Feidh region, maps of the NDVI, NDWI, BI, and SI spectral indices of the study region were developed every 5 years between 1985 and 2020. The diachronic method (Hearn & Álvarez-Mozos, 2021) was adopted to evaluate the dynamics of land use. The principle of this method is based on the comparison of eight multi-date satellite images that cover the 1985–2020 period.

The results from this study will allow us to better understand and appreciate the dynamics of vegetation in the El Feidh perimeter, and to reorient the management of this perimeter. The methodology used in this study is based on different main steps, summarized in the methodological flowchart illustrated in Figure 2.

2.4. Preprocessing of satellite images

Space remote sensing data acquired by the Earth observation system are subject to various radiometric, atmospheric, and geometric errors. These distortions reduce the accuracy of the information extracted and the usefulness of the data.

To optimize the radiometric and geometric aspects of the image to obtain the maximum amount of information, the following corrections must be made:

1. Radiometric correction: eliminate errors generated by sensors that lead to incorrect pixels.
2. Geometric correction: eliminate errors due to satellite movement or errors resulting from the reception mechanism, which cause distortions in the image.
3. Atmospheric correction: eliminate disturbances caused by the presence of dust and gases in the atmosphere, which cause changes in the pixel values of the satellite image.

⁶ It should be noted that the satellite images were chosen between February and May, because these months of Landsat imagery coincide with the growing season of vegetation, particularly of barley grown in the El Feidh perimeter, since the stages of jointing and booting of winter barley in the study area take place between February and April.

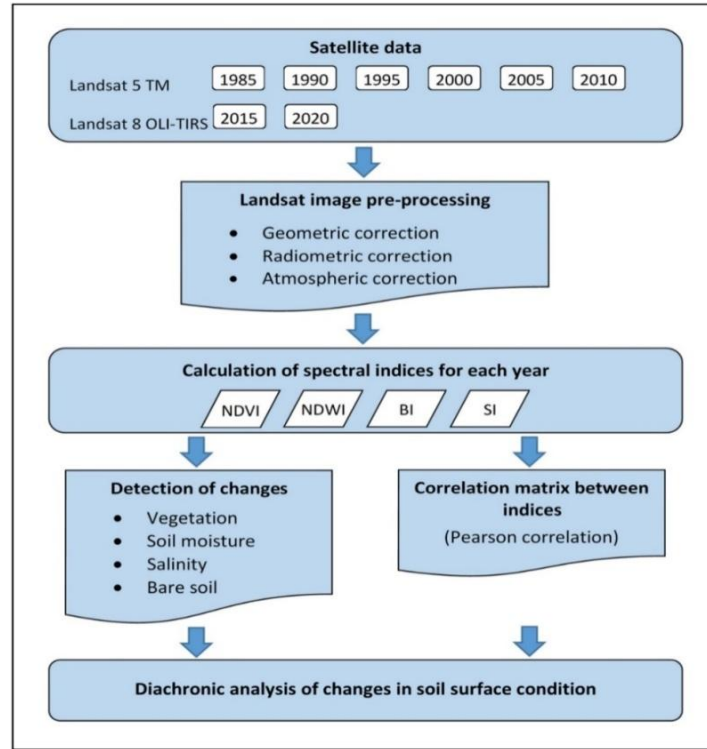


Fig. 2 – Organization chart of the study methodology.

2.5. Choice and calculation of spectral indices

Spectral indices are calculated using a mathematical equation that is applied to two or more spectral reflectance bands of the image. The calculated spectral index is a [new] image that highlights particular features or properties of the land surface, such as vegetation, soil, and water, better than the original input strips. Spectral indices vary from the simple spectral ratio of two bands to more complex combinations of several bands.

NDVI (Normalized Difference Vegetation Index)

The NDVI (Rouse *et al.*, 1974; Tucker, 1979) is a standard vegetation index in the study of vegetation cover (Gao, 1996). This index is calculated using the near-infrared (ρ_{NIR}) and red (ρ_R) electromagnetic bands. The result varies between -1 (other than vegetation, such as water) and 1 (dynamic vegetation). The calculation formula is as follows:

$$NDVI = (\rho_{NIR} - \rho_R) / (\rho_{NIR} + \rho_R) \quad (\text{Eq. 1})$$

Table 2

Formula and description of the selected spectral indices

Spectral index	Formula and description	Reference
NDVI (Normalized Difference Vegetation Index)	$NDVI = (\rho NIR - \rho R) / (\rho NIR + \rho R)$ <ul style="list-style-type: none"> – Sensitive to the vigour and quantity of vegetation – Effective in discriminating the health status of plants 	(Rouse <i>et al.</i> , 1974) (Tucker, 1979)
NDWI (Normalized Difference Water Index)	$NDWI \text{ of Gao} = (\rho NIR - \rho SWIR1) / (\rho NIR + \rho SWIR1)$ <ul style="list-style-type: none"> – Makes it possible to detect water stress in vegetation 	(Gao, 1996)
BI (Bare soil Index)	$BI = \frac{(\rho SWIR1 + \rho R) - (\rho NIR + \rho B)}{(\rho SWIR1 + \rho R) + (\rho NIR + \rho B)} * 100 + 100$ <p style="text-align: center;">$(0 < BI < 200)$</p> <ul style="list-style-type: none"> – Bare soil, fallow land, and vegetation can be identified when using this index 	(Rikimaru <i>et al.</i> , 2002)
SI (Salinity Index)	$SI = \sqrt{\rho B * \rho R}$ <ul style="list-style-type: none"> – Allows the spatial distribution of soil salinity to be evaluated 	(Khan <i>et al.</i> , 2001)

With ρB the spectral band of Blue; ρG the spectral band of Green; ρR the spectral band of Red; ρNIR the Near-Infrared spectral band; $\rho SWIR 1$ and $\rho SWIR 2$ the Mid-Infrared spectral bands (**Note:** the formula bands were chosen based on TM Landsat satellite images).

Bodies of water have negative NDVI values, bare soils have NDVI values close to zero, while areas with dense vegetation have NDVI values varying between 0.6 to +1 (Lillesand & Kieffer, 1994). Nonetheless, numerous researches have demonstrated that NDVI is more or less influenced by humidity conditions and soil colour, particularly in areas with sparse plant cover (Rondeaux *et al.*, 1996; El Bouhissi *et al.*, 2022).

As more than 90% of the spectral information on a plant cover is contained in two bands: red (ρR) and near-infrared (ρNIR), these two bands are most often used to calculate vegetation indices (Baret & Guyot, 1991).

NDWI (Normalized Difference Water Index)

The NDWI from Gao (1996) is an index calculated from the mid-infrared and near-infrared bands. This index detects moisture levels in vegetation, which helps map drought. The NDWI index of Gao is a reliable index of crop water stress, it also makes it possible to check the efficiency of the irrigation system. It must be noted that properly irrigated plants with high water content will reflect an NDWI value close to 1. It was initially proposed to describe the state of vegetation water content over large areas from space: NDWI values over areas of dead grass are negative, while those over areas with green vegetation are positive (Gao, 1996). The NDWI value range is –1 to 1. This index is calculated using the following formula:

$$NDWI \text{ of Gao} = (\rho NIR - \rho SWIR1) / (\rho NIR + \rho SWIR1) \quad (\text{Eq. 2})$$

The NDWI is a measure of liquid water molecules in the plant canopy that interact with incoming solar radiation. This index was designed to estimate canopy water content. NDWI is often a function of local climate and soil properties that control water availability. It is sensitive to changes in liquid water because it incorporates a short-wave infrared band (Serrano *et al.*, 2019).

BI (Bare Soil Index)

The vegetation index value is not as reliable in situations where vegetation covers less than half of the area. For a more reliable estimate of vegetation condition, new methods include a bare soil index

(BI) that is formulated with mid-infrared information. By combining vegetation and bare soil indices in the analysis, the vegetation condition of agricultural land can be assessed (Rikimaru *et al.*, 2002).

The BI index is combined from spectral bands to capture ground variations: blue, red, near-infrared, and shortwave infrared. Short infrared and the red band are used to quantify the mineral composition of the soil, while the spectral bands blue and near-infrared reinforce the presence of vegetation (Loi *et al.*, 2017). The BI index is expressed as a range of values between 0 and 200. The bare soil index is calculated based on this formula:

$$BI = \frac{(\rho_{SWIR1} + \rho_R) - (\rho_{NIR} + \rho_B)}{(\rho_{SWIR1} + \rho_R) + (\rho_{NIR} + \rho_B)} * 100 + 100$$

(0 < BI < 200) **(Eq. 3)**

SI (Salinity Index)

Several studies over the past 30 years were conducted to monitor soil salinity using remote sensing (Metternicht & Zinck, 2003; Dehni & Lounis, 2012; Sahbeni *et al.*, 2023). A number of these studies highlighted the relationship between salinity and the spectral reflectance of soil components, which revealed that salt crusts deposited on the surface of soils show strong reflectance in the visible and near-infrared bands (Singh & Sirohi, 1994; Schmid *et al.*, 2008). These studies use either methods based on the classification of satellite images (Allbed & Kumar, 2013) or index approaches (Khan *et al.*, 2001; Khan *et al.*, 2005; Douaoui *et al.*, 2006; Bannari *et al.*, 2008). To detect salinity in this arid ecosystem, we used a salinity index that was proposed by Khan *et al.* (2001). There is no specific range for SI values, but they are always positive (greater than 0):

$$SI = \sqrt{\rho_B * \rho_R}$$

(Eq. 4)

Statistical analysis (Pearson correlation)

The Pearson correlation coefficient is an index that reflects the linear relationship between two continuous variables. The coefficient varies between -1 and $+1$; a value of 0 indicates no linear relationship between the variables. A negative value (negative correlation) means that as one variable increases, the other decreases, while a positive value (positive correlation) indicates that both variables increase or decrease alongside each other. In this study, Pearson's correlation coefficient was used to measure the linear relationship between all variables (NDVI, NDWI, BI, and SI). IBM SPSS Statistics software (version 22) was used for the calculations.

3. RESULTS

3.1. Spectral indices

As part of this research, various spectral indices were calculated to study the vegetation cover (NDVI), humidity (NDWI), bare soil (BI), and salinity (SI) of the El Feidh irrigation perimeter.

NDVI

NDVI has been widely used to examine the relationship between vegetation spectral variability and changes in vegetation growth rate. The results of this study revealed a gradual decrease in average pixel NDVI values over the years, from the highest value of 0.49 recorded in 1985 to the lowest value of 0.12 in 2020.

Figure 3 and Table 3 show the area of vegetation density classes according to NDVI in the irrigation perimeter from 1985 to 2020: In 1985, the highest values of the NDVI (greater than 0.3) were distributed almost over the entire perimeter (71.81%), with the exception of agricultural land located in the North and South where the values of the NDVI are under 0.3. However, in 1990, the highest NDVI values (greater than 0.3) were focused at the centre of the irrigation perimeter (23.94% of the perimeter).

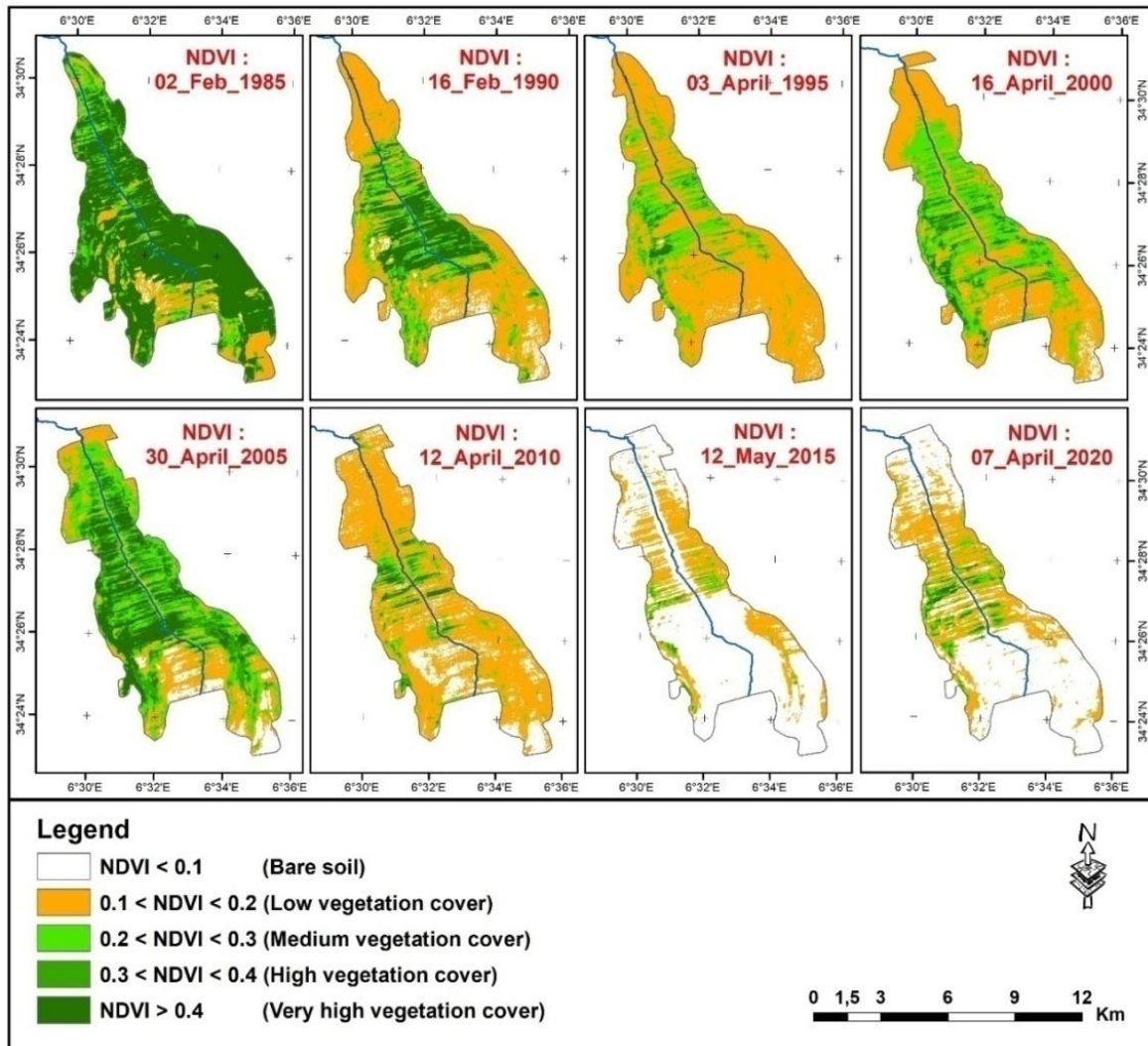


Fig. 3 – Spatial variation of vegetation cover, according to the NDVI index from 1985 to 2020 (Sahebjalal & Dashtekian, 2013).

Table 3

Evolution of density classes of the NDVI index between 1985 and 2020

Year	Interval	Vegetation density	Surface (Km ²)	Percentage (%)	Year	Interval	Vegetation density	Surface (Km ²)	Percentage (%)
1985	0.058–0.1		–	–	2005	0.055–0.1		–	–
	0.1–0.2	Low	7.366	14.16		0.1–0.2	Low	14.505	24.82
	0.2–0.3	Medium	6.717	12.92		0.2–0.3	Medium	16.015	27.40
	0.3–0.4	High	6.768	13.01		0.3–0.4	High	12.538	21.45
	0.4–1.144	Very high	30.579	58.80		0.4–0.796	Very high	11.245	19.24
Total			51.430	98.89	Total			54.303	92.91
1990	0.068–0.1		–	–	2010	0.065–0.1		–	–
	0.1–0.2	Low	27.057	52.03		0.1–0.2	Low	42.402	71.92
	0.2–0.3	Medium	9.969	19.17		0.2–0.3	Medium	5.050	8.57
	0.3–0.4	High	5.177	9.95		0.3–0.4	High	1.917	3.25
	0.4–0.917	Very high	7.275	13.99		0.4–0.712	Very high	1.090	1.85
Total			49.478	95.14	Total			50.459	85.59
1995	0.072–0.1		–	–	2015	0.046–0.1		–	–
	0.1–0.2	Low	38.518	73.41		0.1–0.2	Low	14.744	24.58
	0.2–0.3	Medium	10.616	20.24		0.2–0.3	Medium	2.024	3.38
	0.3–0.4	High	2.088	3.98		0.3–0.4	High	0.518	0.86
	0.4–0.697	Very high	0.494	0.94		0.4–0.477	Very high	0.040	0.07
Total			51.716	98.57	Total			17.326	28.89
2000	0.080–0.1		–	–	2020	0.050–0.1		–	–
	0.1–0.2	Low	30.224	52.96		0.1–0.2	Low	19.866	32.90
	0.2–0.3	Medium	18.873	33.07		0.2–0.3	Medium	3.837	6.36
	0.3–0.4	High	5.176	9.07		0.3–0.4	High	1.488	2.46
	0.4–0.678	Very high	1.498	2.62		0.4–0.683	Very high	0.761	1.26
Total			55.771	97.72	Total			25.952	42.98

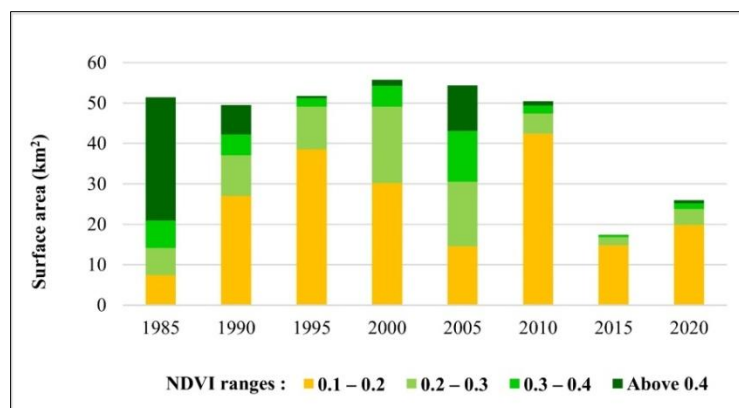


Fig. 4 – Variation in vegetation density between 1985 and 2020.

It can be noticed that during the year 2000, the highest NDVI values (which are greater than 0.3) make up only 11.69% of the perimeter, while the average values of the NDVI index (between 0.2 and 0.3) account for just 33.07% of the perimeter surface.

However, during 2010, the irrigation perimeter suffered a significant decrease in the NDVI. It is the values between 0.1 and 0.2 that dominate, with a percentage of 71.93% of the perimeter surface. On the other hand, the NDVI values that are greater than 0.3 only represent 5.10% of the perimeter.

Nonetheless, during the year 2020, the NDVI vegetation index values of the study area decreased significantly: NDVI values greater than 0.3 represent only 3.72%, while NDVI values that vary between

0.2 and 0.3 make up 6.36% of the perimeter, and NDVI values belonging to the [0.1–0.2] interval account for 32.90% of the total perimeter area.

It can be concluded that the El Feidh perimeter experienced a decline in the NDVI index during the study period (1985–2020), particularly starting in 2015. The results indicate a significant decrease in the average NDVI value of pixels over the years. In 1985, the average NDVI was 0.49, which then dropped to 0.17 in 1995, before rising to 0.28 in 2005. However, after this year, the NDVI continued to decline, reaching 0.12 in 2020. This degradation, especially between 2010 and 2015, is largely attributed to the reduced flood flows from Oued El Arab.

NDWI

The results of changes in the NDWI index for different time intervals are shown in Figure 5. It is obvious that the average value of NDWI regarding pixels has continuously decreased from 0.19 in 1985 to -0.08 in 2020.

According to NDWI results, it is noticeable that the year 1985 was the best one, as the NDWI in the [0.3–0.6] interval took up 17.941 km² (34.50%). Further analysis of the year 1985 reveals that the NDWI in the [0.5–0.6] interval is characterized by moderate moisture content, taking over an area of 4.864 km² (9.35%).

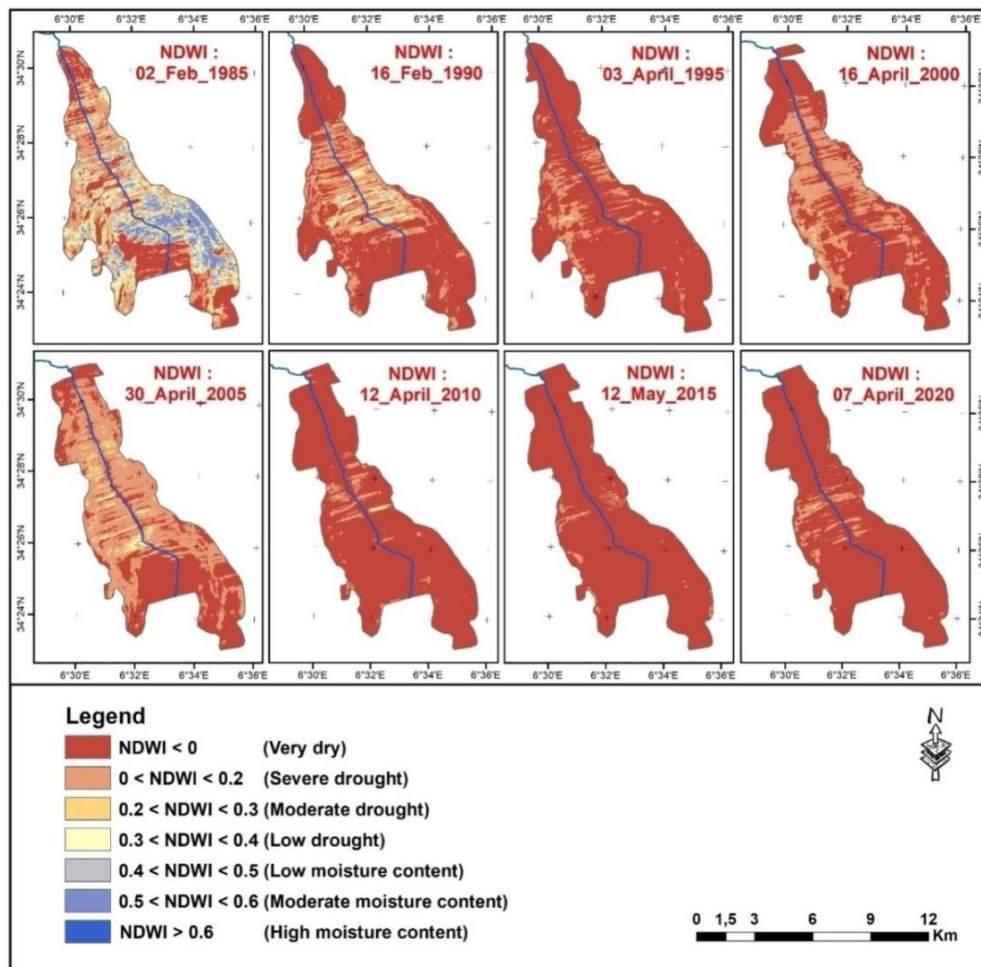


Fig. 5 – Spatial variation of humidity according to the NDWI index from 1985 to 2020 (Gulácsi & Kovács, 2015).

Another noteworthy aspect is the period between 1990 and 2000, when the predominance of the NDWI interval was under 0 (this interval is characterized by a very strong drought). The results show the percentages of areas covered by this interval: (67.52% in 1990 and 87.94% in 1995 and, finally, 68.55% in 2000). Later on, in 2005, the NDWI interval, which stands out due to severe drought (0–0.2), is dominant, covering an area of 29.073 km² (49.74%). Finally, between 2010 and 2020, we observe a total predominance of the NDWI interval under 0 (characterized by a very strong drought). This interval includes the following areas: 94.64% in 2010, 97.56% in 2015, and 94.46% in 2020.

BI

According to the results of the BI index, we note that values above 110 indicate that the soils are bare, while values below 110 indicate that the lands are covered in vegetation. The perimeter of El Feidh has undergone four stages between 1985 and 2020, as illustrated in Figure 6.

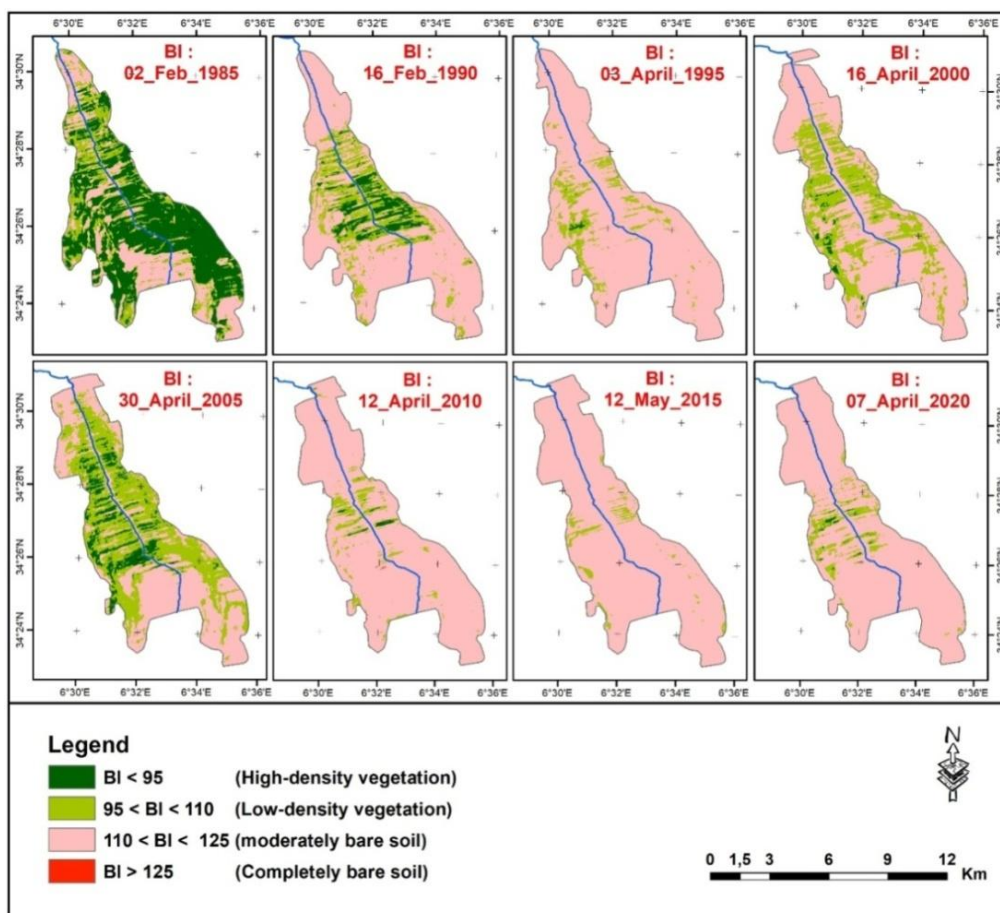


Fig. 6 – Spatial variation of land use according to the BI index from 1985 to 2020.

In 1985, bare soil made up only 27.94% of the perimeter, but vegetation took up 72.06%. Then, between 1990 and 2000, bare soil surfaces increase slightly, the average of these surfaces during this period is 76.57%. However, in 2005, the perimeter situation improved, mainly due to the decrease in bare soil, which accounts for 46.24% of the perimeter, while the rest of the land was covered in vegetation (53.76%). Finally, between 2010 and 2020, bare soils were the most prevalent; it is also noteworthy that the average surface area of bare soils during this period was 93.89%.

SI

The results summarized in Figure 7 show that the average SI value of the pixels increases over the years. In 1985, the average SI of pixels was 952.04. After that, it increased to 1,915.44 in 2000, and again to 2,261.63 in 2020.

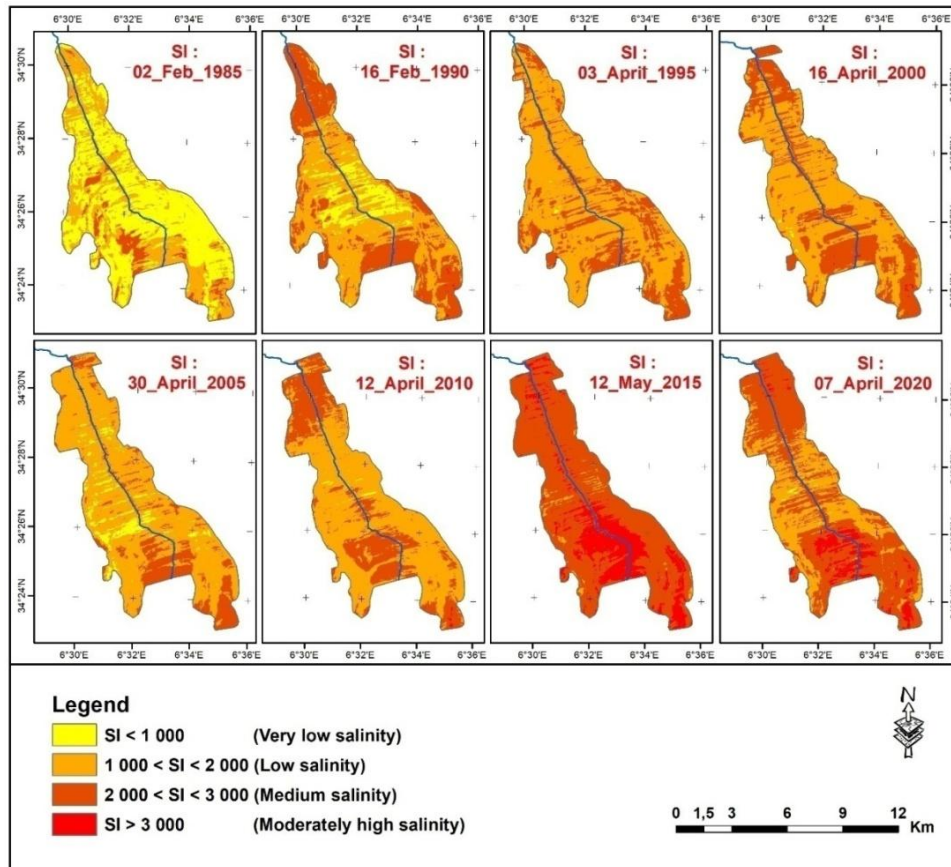


Fig. 7 – Spatial variation of salinity according to the SI index from 1985 to 2020.

Then, between 1990 and 2010, the [1,000 to 2,000] interval characterized by low salinity is dominant (53.11% in 1990; 69.70% in 1995; 60.51% in 2000; 75.61% in 2005 and 66.75% in 2010).

Finally, between 2015 and 2020, the salinity [2,000 – 3,000] interval (characterized by average salinity) became the dominant one. In 2015, this interval covered 45.225 km² (75.41%) of the study area and then decreased to 35.922 km² (59.50%) in 2020.

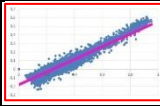
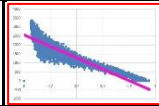
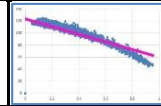
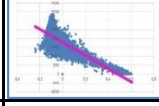
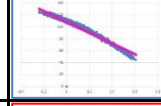
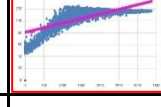
3.2. Pearson correlation matrix between indices

The Pearson correlation analysis was used to test the relationships between NDVI, NDWI, BI, and SI during the 1985–2020 period. The results are summarized in Table 4.

All correlations are statistically significant at $P < 0.01$. The results showed a positive correlation between NDVI and NDWI ($R = 0.961$) and between SI and BI ($R = 0.724$). However, there was a negative correlation between NDVI and SI ($R = -0.839$), NDVI and BI ($R = -0.793$), NDWI and SI ($R = -0.751$), and between NDWI and BI ($R = -0.862$). Nevertheless, in this study, we focused only on 3 correlations:

Table 4

Pearson correlation matrix between the different indices

		NDVI (1985 – 2020)	NDWI (1985 – 2020)	SI (1985 – 2020)	BI (1985 – 2020)
NDVI (1985–2020)	Pearson correlation	1			
	Sig. (bilateral)				
	N	8003			
NDWI (1985–2020)	Pearson correlation	0.961 **	1		
	Sig. (bilateral)	0.000			
	N	8003	8003		
SI (1985–2020)	Pearson correlation	-0.839 **	-0.751 **	1	
	Sig. (bilateral)	0.000	0.000		
	N	8003	8003	8003	
BI (1985–2020)	Pearson correlation	-0.793 **	-0.862 **	0.724 **	1
	Sig. (bilateral)	0.000	0.000	0.000	
	N	8003	8003	8003	8003

** The correlation is significant at the 0.01 level (bilateral).

Regarding the correlation between the NDVI and the NDWI, it was a very strong positive one ($R = 0.961$), which can be explained by water, the main limiting factor for primary production in arid and semi-arid regions. Water availability directly influences vegetation growth, making these two indices strongly correlated.

Concerning the correlation between NDVI and SI, the results showed that there was a moderate negative correlation between NDVI and SI values ($R = -0.839$), which confirms that changes in vegetation cover are closely related to changes in soil salinity.

For the correlation between SI and BI, it is noted that there was a moderate positive correlation between soil salinity and bare soils at ($P < 0.01$) with a correlation of $R = 0.724$.

4. DISCUSSIONS

4.1. Indices

NDVI

The Normalized Difference Vegetation Index (NDVI) has been used in several global and regional studies. The objective of this index was to monitor the evolution of vegetation, particularly in vulnerable areas. As the index was determined using a normalization process, NDVI values varied between 0 and 1, indicating sensitive responsiveness to green vegetation even in places with little plant cover.

In Algeria, the area of land benefiting from flood spreading has decreased over the years; it was estimated to be 110,000 ha in 1984 (FAO, 1995), then dropped to 56,050 ha in 2001 (FAO, 2005), only to slightly decrease yet again to 53,000 ha in 2008 (FAO, 2015a). In Morocco, it has also been observed that the land irrigated by cruse water has shrunk over the years: the surface area was 165,000 ha in 1989 (FAO, 1995), and then dropped to 62,200 ha in 2011 (FAO, 2015b). These figures show a decrease in the area of spate irrigation perimeters in Algeria and Morocco, as well as a clear decrease in the NDVI of the El Feidh perimeter over the study period (1985-2020), which suggests the degradation of spate irrigation perimeters in semi-arid zones.

The results revealed an abundance of plant cover within the El Feidh perimeter in 2000, and especially in 2005, despite the reduction in flood waters due to the construction of Babar Dam in 1995.

This situation can be explained by the partial exploitation of the dam between 2002 and 2013 (Tebbi, 2014).

NDWI

Conventionally, Normalized Difference Water Index (NDWI) values range from -1 to +1. Positive values correspond to dense vegetation with high water content, while negative values indicate areas with a low vegetation cover or dead vegetation. The NDWI makes it possible to detect vegetation when it is in a state of water stress. Therefore, it is useful for monitoring vegetation in the context of climate change.

Analysis of NDWI maps between 1985 and 2020 shows a sharp decrease in the NDWI index. This decline is obviously caused by the construction of Babar Dam upstream of the El Feidh perimeter.

The A.N.R.H.⁷ data over the ten years in operation (2002-2013) show that Babar Dam received a volume of 260 hm³, of which 29% was discharged by the flood spillway (75.4 hm³). On the other hand, the water evacuated by the bottom drain is estimated at 27% (70.2 hm³) during the 2002-2013 period, knowing that the bottom drain technique is used during flood periods. These data show that 56% of water was evacuated during floods from 2002 to 2013, which allowed farmers to better irrigate the El Feidh perimeter in 2005 and 2010. Based on these data, and to ensure the sustainability of the El Feidh irrigation system in the future, coordination and joint management must be established between Babar Dam and the El Feidh perimeter.

BI

The Bare Soil Index (BI) can determine the difference between vegetation and bare soil. When using the BI index, we can differentiate between bare soil, fallow land and vegetation. According to Doumit & Sakr (2015), the value of this index is not very reliable in the area with dense vegetation, but in the Bekaa Valley (Lebanon), the results of this index were very reliable for the delimitation of bare lands and urbanization.

In the spate irrigation perimeter of El Feidh, the results of this index are deemed reliable for the delimitation of bare soil and land covered in vegetation.

SI

Generally, two types of salinization have been identified: primary (natural) salinization and secondary salinization. The first occurs during the alteration of salified rocks or due to natural external contributions. In contrast, the second one (secondary salinization) is caused by human activities that are frequently linked to inappropriate agricultural practices. According to Djili *et al.* (1999) and Legros *et al.* (2009), there are four major causes for the secondary salinization of agricultural land: the use of poor-quality irrigation water, insufficient water to leach salts, poor soil drainage, and the rise of the water table.

Owing to the high demand for food products, the percentage of irrigated land has increased over the past thirty years, leading to an increase in salinized land. In Pakistan, more than 25% of irrigated soils suffer from salinization, 25% in Tunisia, 23% in the United States, about 17% in India, approximately 15% in China, and around 9% in South Africa (IPTRID, 2006). In Algeria, the surface area of saline land is estimated today at 1.5 million hectares, of which 49,000 ha are located in the south of the country (Abdelhafid, 2010), based on the fact that salinization affects approximately 20% of irrigated agricultural land in the country (Douaoui & Hartani, 2008).

According to the soil map of Tébessa (Barbut & Durand, 1938), the perimeter of El Feidh is naturally and completely classified as saline soils (Solonchaks⁸), given that the evolution of these soils is due to the excessive presence of soluble salts, which results in unfavourable chemical, physical, and biological properties. In addition, these soluble salts have harmful effects on soil and vegetation.

⁷ National Agency for Hydraulic Resources (In French: Agence Nationale des Ressources Hydrauliques).

⁸ Solontchak is a type of soil with high salinity, formed when evaporation exceeds rainfall input.

In this study area, the waters of Oued El Arab are characterized by an average salt content, but the quality of these waters exceeds international standards. The water of the river is hard to very hard and has an encrusting character (Khadraoui & Taleb, 2008).

In general, the most frequent causes of salinity in the lands of the El Feidh spate irrigation perimeter are the high contributions of mineral matter from the waters of Oued El Arab, as well as the low leaching of agricultural land (insufficient water), together with the high evapotranspiration recorded within the perimeter of El Feidh (2,498 mm).

4.2. Correlations

Correlation between NDVI and NDWI

A very strong and significant positive correlation was found between NDVI and NDWI ($R = 0.961$), so that our results are in agreement with those obtained by Wgnn & Vmi (2020), as well as by Serrano *et al.* (2019).

The study by Wgnn & Vmi (2020) analysed multi-temporal and non-temporal agricultural drought indices calculated using the indices NDVI, NDWI, and LST⁹. The authors studied the sensitivity of drought indices for monitoring agricultural droughts and cropping conditions in the dry zone rainfed rice cultivation in Sri Lanka and found that vegetation greenness (NDVI) and vegetation water content (NDWI) are strongly correlated ($R = 0.89$).

According to Wgnn & Vmi (2020), the scientists verified the ability of NDVI and NDWI to represent crop stress and concluded that the relationship between satellite-derived vegetation indices and soil moisture strongly depends on land cover heterogeneity and soil type. Scientists have suggested that both indices are suitable for monitoring water stress on vegetation but have recommended a further sensitivity analysis for different geographic regions.

On the other hand, Serrano *et al.* (2019) carried out a study to evaluate the NDWI index as a tool to monitor the seasonal and interannual variability of pastures in a Mediterranean agro-silvo-pastoral system (in the South of Portugal). The authors showed that there was a strong and significant correlation between NDVI and NDWI ($R = 0.93$ with $P < 0.01$), as observed in other studies as well (e.g., Gao, 1996; Gu *et al.*, 2008).

The water content index (NDWI) is sensitive to changes in the liquid water content of vegetation. However, this cannot be considered a replacement for NDVI, but rather as a complementary aspect, as proposed by Gao (1996).

Correlation between NDVI and SI

The results of this study showed a moderate and significant negative correlation ($R = -0.839$) between plant cover and soil salinity in the El Feidh spate irrigation perimeter. Our results are consistent with those obtained by Al-Khakani & Yousif (2019), who evaluated and detected changes in soil salinity and plant cover in part of the An-Najaf governorate. The correlation values between NDVI and SI calculated by these authors were $R = -0.94$ for the 2001 – 2009 period, and $R = -0.92$ for the 2009 – 2015 period, with $P < 0.0001$ for both periods.

According to Al-Khakani & Yousif (2019), the soil salinity levels of An-Najaf experienced notable changes during the study period. This may be due to the increase in temperature and a decrease in average precipitation, which have led to high evaporation, in addition to poor irrigation systems and poor land use, all of which contributed to the increase in the soil salinity levels in An-Najaf.

In the spate irrigation perimeter of El Feidh, the results indicated a significant reduction in plant cover associated with an increase in salinity levels. Average pixel NDVI values decreased by 24.49%, whereas the average SI values of the pixels increased by 237.56%. The correlation result for the El Feidh perimeter showed that there is an inverse relationship between NDVI and SI values ($R = -0.839$), which confirms that changes in vegetation cover are strongly connected to changes in soil salinity.

⁹ Land Surface Temperature (LST).

Correlation between SI and BI

In the study area, the correlation results showed that there is a moderate positive correlation ($R = 0.724$) between the salinity index (SI) and the bare soil index (BI). This correlation confirms that soil salinity is generally higher in bare soils and lower in lands covered by vegetation.

Alqasemi *et al.* (2021) developed a model to estimate and monitor soil salinity in Abu Dhabi (United Arab Emirates) using remote sensing-based spectral indices and soil salinity field measurements. The authors found a moderate positive correlation of 0.64 between the salinity index (SSI1) and the bare soil index (BSI)¹⁰, a result similar to that of our study.

There are several studies that have addressed the correlation between the measured salinity (EC) and the salinity index. For example, authors Douaoui & Yahiaoui (2015) evaluated the salinity indices of bare soils in the El Hmadna plain¹¹ where they noticed a strong correlation of 0.86 between the measured salinity (EC) and the salinity index (SIH), because the period of their study (June 2010) coincided with a very low (or non-existent) vegetation cover with a significant accumulation of salts, which facilitated the detection of salts.

In contrast, Abdennour (2021) noted a weak correlation between measured salinity (EC) and salinity indices in the well-watered oases of El Ghrous (Wilaya of Biskra). Knowing that the recorded correlation coefficients were between 0.02 and 0.11, these weak correlations can be explained by two factors: (i) the field measurements were taken on cultivated and irrigated land, which may not fully represent natural conditions, and (ii) the decrease in soil salinity was caused by the leaching of the upper soil layer due to irrigation, which complicates the detection of salinity levels.

4.3. General discussion

The negative effect of Babar Dam

Babar Dam, stretching over an area of 567 km², was built on the Oued El Abiod to retain the waters of Oued Tamagra to the West and Oued El Hatiba to the East (Gaagai *et al.*, 2020). The dam was filled with water in 1995 and regulated an annual volume of 12 hm³. According to Guidoum (2017), the volume of water mobilized (41 hm³) was initially intended to irrigate farms in eastern Ziban (the agricultural perimeter of Kheirane and the lands developed upstream). After the construction of Babar Dam, the low residual flow downstream of the Oued El Arab is far from meeting the water needs of the 30,000 palm trees located in the commune of Khangat Sidi Nadji and the spate irrigation perimeters.

Oued El Arab offers the largest flow of all *oueds* of southern Aurès ($Q = 0.71 \text{ m}^3/\text{s}$)¹² (Mebarki, 2005). On the other hand, the average annual flow that supplies Babar Dam is 0.39 m³/s (flow estimated by the Samie formula). Therefore, the average annual flow that remains in Oued El Arab is estimated at approximately 0.32 m³/s (calculated value). This new situation has harmful effects on the spate irrigation perimeter of the El Feidh region (Fig. 8) because the water resources of the Oued El Arab have been halved since 1995.

Climate change in Algeria

Climate change is primarily caused by the emission of gases such as carbon dioxide (CO₂), which trap the Sun's heat in the Earth's lower atmosphere, leading to an increase in Earth's temperature known as global warming (Thirukanthan *et al.*, 2023).

The Maghreb has been considered a region particularly vulnerable to risks linked to climate change. In Algeria, climate change is a major concern. Due to its geographical position, Algeria is exposed to the negative effects of climate change and greenhouse gas emissions (GHG), including drought, high temperatures, and floods. According to Farah (2014), a comparison of climatic elements in Algeria between the 1931–1960 and 1961–1990 periods rendered the following results:

¹⁰ The bare soil index (BSI) used by these authors has the same formula as that used in this study.

¹¹ The Hmadna plain is located in the western part of the Cheliff plains (Northwest Algeria).

¹² This flow is calculated based on the average annual flow rates for the period: 1972/73-1993/94.

- An average decrease of 10% in precipitation.
- An increase in temperature of approximately 0.5°C.
- The water deficit is greater in the West of the country than in the Central and Eastern parts.



Fig. 8 – Floodwater diversion channels in the El Feidh perimeter.
 Source: The authors, May 2022.

On the other hand, according to the same author (2014), a study by the O.N.M.¹³ revealed that there was a 12% decline in precipitation for the 1990–2005 period compared to the 1961–1990 period, leading to widespread drought at the same time as other regions are experiencing floods.

In the long term, adaptive processes may be the most effective mechanisms for coping with drought. Proper irrigation use, changes in plant varieties and in land management practices are among the most featured adaptation measures. They are necessary to reduce (agro-)ecosystem sensitivity to these extreme events and to avoid ecological, economic, as well as social losses (Sultan & Djellouli, 2013; Thibaut & Ozer, 2021).

Difficulties and prospects of the irrigation perimeter

*** Yield**

Generally, the dynamics of vegetation in the El Feidh area are strongly influenced by the frequency of floods. There is a relationship between the number of floods and the yield in the El Feidh area: if during the winter there is only one flood event, grains¹⁴ will be harvested while green, and will serve as fodder for the livestock; two flood events ensure a correct grain harvest, three flood events well-distributed over time may yield more than 50 quintals per hectare: the income is shared between the members of the fraction according to the laws of the community. Thus, in 1985, an exceptional year in terms of rainfall, yields of 80 quintals per hectare were observed in the El Feidh irrigation area (Côte, 2008), unthinkable yields for northern Algeria.

*** Decrease in irrigated land**

There has been a reduction in irrigated areas, which went from around 5,000 ha in 1985 to 2,500 ha in 2020. This low rate of areas irrigated by spate irrigation can be explained by three factors:

- Unfavourable rainfall and a prolonged dry season.
- Babar Dam (after its impoundment).
- The observation of the flood in real time, its quantification, the estimation of the spreading areas, and the interest given to this measurement campaign are all assets for a good approach.

¹³ National Meteorological Office (In French: Office National de la Météorologie).

¹⁴ Barley and wheat.

* Maintenance

The flood diffusion channels of the *oued* and the irrigation water distribution channels require regular monitoring and maintenance, particularly after each flood. Although the construction of these perimeters was spread over several generations, it was nevertheless necessary for each of them that the beneficiaries share a common interest in order to guarantee maintenance. A central authority capable of coordinating development and maintenance work, regulating an equitable distribution of water, and guaranteeing the rights of each is then necessary for the proper functioning of the system. Although land and water management were based on the community, it was nevertheless necessary for it to have, at the local level, sufficient power to organize the work and maintenance of the structures.

* Water management

Before the construction of Babar Dam, farmers in the El Feidh area benefited from the major floods of Oued El Arab, but after the construction of this dam, the situation changed where the major floods were stored in the dam. This is why it is recommended that those responsible for Babar Dam periodically release water through the bottom drain to ensure the irrigation of the El Feidh irrigation area. For the sustainable management of the El Feidh area, it is necessary to dig boreholes inside the irrigation area because there are successful experiences of farmers who have dug boreholes on agricultural lands close to the irrigation area.

5. CONCLUSIONS

This study focuses on the calculation of spectral indices (NDVI, NDWI, BI, and SI) for the diachronic monitoring of changes in the surface state of soils in a spate irrigation perimeter of an arid environment in the region of El Feidh, by exploiting Landsat satellite images (TM and OLI-TIRS) over the 1985 – 2020 period. The results indicate that the satellite images used for change detection can provide appropriate information on changes in land cover vegetation, humidity of agricultural land, soil salinity, and surface area of bare soil.

Monitoring changes in the vegetation cover using NDVI data shows that the El Feidh perimeter has experienced a progressive decrease in cultivated area, as well as a reduction in vegetation density. In 1985, the average NDVI pixel value was 0.49, which then dropped to 0.20 in 2000, only to finally reach 0.12 in 2020. The analysis of changes in the NDWI revealed a significant decrease in soil and vegetation humidity during the study period. The average NDWI of pixels was 0.19 in 1985, then dropped to -0.03 in 2000, only to continue to decrease to -0.08 in 2020.

Simultaneously, the salinity index gradually increased. The [0 – 1,000] interval was dominant in 1985, to be followed by the [1,000 – 2,000] interval which predominated from 1990 to 2010. Finally, the [2,000 – 3,000] interval was dominant from 2015 to 2020.

Monitoring the BI index pointed to an increase in the area of bare soil over the years. In 1985, bare soil made up only 27.94% of the perimeter, while the rest (72.06%) was taken up by vegetation. The proportion of bare soil exceeded 60% between 1990 and 2000. In 2005, this proportion decreased slightly to 46.24%; however, between 2010 and 2020, bare soils increased considerably, exceeding 90% of the perimeter of El Feidh.

Regarding the El Feidh perimeter, a very strong and significant positive correlation was observed between the greenness of vegetation (NDVI) and the water content of vegetation (NDWI) [R = 0.961]. On the other hand, there was a moderate negative correlation between vegetation cover (NDVI) and soil salinity (SI) [R = -0.839], as well as a moderate positive correlation between soil salinity (SI) and the presence of bare soil (BI) [R = 0.724].

The main factor contributing to the regression of the El Feidh perimeter is Babar Dam, built in 1995 on Oued Abiod, which blocked the flow of water towards the Oued El Arab. Before 1995, the flow

of Oued El Arab was 0.71 m³/s, but after 1995, it decreased by 54.93%. In addition, the effects of climate change in Algeria have contributed to a reduction in the area of vegetation cover in the El Feidh perimeter. A comparison of rainfall in Algeria between the 1931–1960 and 1961–1990 periods indicates an average decrease of 10%, while a comparison between the 1961–1990 and 1990–2005 periods reveals a decrease of 12%.

The use of very high spatial resolution (THRS) satellites (such as QuickBird, Ikonos, etc.) to track parameters such as NDVI and soil salinity could improve this type of analysis in the future, which bolsters the idea that further studies on the subject are more than necessary.

Acknowledgements

Our sincere thanks go to the General Directorate of Scientific Research and Technological Development (DGRSDT) for its support, as well as to our family, colleagues, and friends for their encouragement. We would also like to express our gratitude to NASA¹⁵ for providing free satellite images without which this research would not have been carried out. Last but not least, we would like to thank Frères Mentouri University (Constantine 1), which encouraged us to address this topic.

REFERENCES

- Abdelhafid, Y. (2010), *Cartographie de la salinité des sols par induction électromagnétique: cas de la zone Est du périmètre irrigué de la Mina*. Thèse de magister, École nationale supérieure agronomique (ENSA) d'El Harrach – Alger, 102 p.
- Abdennour, M. A. (2021), *Variabilité spatio-temporelle de la salinisation des sols du périmètre irrigué du Ziban (Biskra) – Apport de la géostatistique et de la télédétection*. Thèse de doctorat, Université Mohamed Khider de Biskra, 127 p.
- Alexandridis, T. K., Zalidis, G. C., Silleos, N.G. (2008), *Mapping irrigated area in Mediterranean basins using low cost satellite Earth Observation*. Computers and Electronics in Agriculture, **64**(2), pp. 93–103.
- Alexandridis, T. K., Panagopoulos, A., Galanis, G., Alexiou, I., Cherif, I., Chemin, Y., Stavrinou, E., Bilas, G., Zalidis, G. C. (2014), *Combining remotely sensed surface energy fluxes and GIS analysis of groundwater parameters for irrigation system assessment*. Irrigation Science, **32**, pp. 127–140.
- Al-Khakani, E. T., Yousif, S. R. (2019), *An assessment of soil salinity and vegetation cover changes for a part of An-Najaf governorate using remote sensing data*. Journal of Physics: Conference Series **1234**: 012023. IOP Publishing.
- Allbed, A., Kumar, L. (2013), *Soil salinity mapping and monitoring in arid and semi-arid regions using remote sensing technology*. Advances in Remote Sensing, **2**(4), pp. 373–385.
- Alqasemi, A. S., Ibrahim, M., Fadhil Al-Quraishi, A. M., Saibi, H., Al-Fugara, A., Kaplan, G. (2021), *Detection and modeling of soil salinity variations in arid lands using remote sensing data*. Open Geosciences; **13**(1), pp. 443–453.
- Ambast, S. K., Keshari, A. K., Gosain, A. K. (2002), *Satellite remote sensing to support management of irrigation systems: concepts and approaches*. Irrigation and Drainage, **51**(1), pp. 25–39.
- Athamena, A., Gaagai, A., Aouissi, H.A., Burlakovs, J., Bencedira, S., Zekker, I., Krauklis, A.E. (2023), *Chemometrics of the Environment: Hydrochemical Characterization of Groundwater in Lioua Plain (North Africa) Using Time Series and Multivariate Statistical Analysis*. Sustainability **15**(1), 20.
- Atzberger, C. (2013), *Advances in remote sensing of agriculture: Context description, existing operational monitoring systems and major information needs*. Remote Sensing, **5**(2), pp. 949–981.
- Bannari, A., Guedon, A. M., El-Harti, A., Cherkaoui, F. Z., El-Ghmari, A. (2008), *Characterization of slightly and moderately saline and sodic soils in irrigated agricultural land using simulated data of advanced land imaging (EO-1) sensor*. Communications in Soil Science and Plant Analysis, **39**(19-20), pp. 2795–2811.
- Barbut, M., Durand, J-H. (1938), *Carte des sols d'Algérie*. Mascara. Feuille N.I. 31-N.O. Service Géographique de l'Armée.
- Baret, F., Guyot, G. (1991), *Potentials and limits of vegetation indices for LAI and APAR assessment*. Remote Sensing of Environment, **35**(2-3), pp. 161–173.
- Bastiaanssen, W. G. M., Bos, M. G. (1999), *Irrigation performance indicators based on remotely sensed data: a review of literature*. Irrigation and Drainage Systems, **13**(4), pp. 291–311.
- Bastiaanssen, W. G. M., Molden, D. J., Makin, I. W. (2000), *Remote sensing for irrigated agriculture: examples from research and possible applications*. Agricultural Water Management, **46**(2), pp. 137–155.
- Bastiaanssen, W. G. M., Ali, S. (2003), *A new crop yield forecasting model based on satellite measurements applied across the Indus Basin, Pakistan*. Agriculture, Ecosystems and Environment, **94**(3), pp. 321–340.

¹⁵ <https://earthexplorer.usgs.gov/>.

- Bid, S. (2016), *Change detection of vegetation cover by NDVI technique on catchment area of the Panchet Hill Dam, India*. International Journal of Research in Geography, **2**(3), pp. 11–20.
- Biggs, T. W., Thenkabail, P. S., Gumma, M. K., Scott, C. A., Parthasaradhi, G. R., Turrall, H. N. (2006), *Irrigated area mapping in heterogeneous landscapes with MODIS time series, ground truth and census data, Krishna Basin, India*. International Journal of Remote Sensing, **27**(19), pp. 4245–4266.
- Brookfield, A. E., Zipper, S., Kendall, A. D., Ajami, H., Deines, J. M. (2024), *Estimating Groundwater Pumping for Irrigation: A Method Comparison*. Groundwater, **62**(1), pp. 15–33.
- Côte, M. (1998), *Les régions bioclimatiques de l'Est algérien*, Rhumel, **6**, pp. 57–71.
- Côte, M. (2008), *Pays, paysages, paysans d'Algérie*, Éditions Média-Plus, Constantine, 282 p.
- Dadhwal, V. K., Singh, R. P., Dutta, S., Parihar, J. S. (2002), *Remote sensing based crop inventory: A review of Indian experience*. Tropical Ecology, **43**(1), pp. 107–122.
- Dehni, A., Lounis, M. (2012), *Remote sensing techniques for salt affected soil mapping: application to the Oran region of Algeria*. Procedia Engineering, **33**, pp. 188–198.
- Djili, K., Daoud, Y., Ayache, N. (1999), *Analyse de la distribution verticale et spatiale du calcaire dans les sols de l'Algérie septentrionale*. Étude et Gestion des Sols, **6**(3), pp. 201–214.
- Douaoui, A.E.K., Nicolas, H., Walter, C. (2006), *Detecting salinity hazards within a semiarid context by means of combining soil and remote-sensing data*. Geoderma, **134**(1-2), pp. 217–230.
- Douaoui, A.E.K., Hartani, T. (2008), *Impact de l'irrigation par les eaux souterraines sur la dégradation des sols de la plaine du Bas-Chéliff*, in *Economies d'eau en systèmes irrigués au Maghreb* (coord. Kuper, M., & Zaïri, A.), Actes du troisième atelier régional du projet Sirma, Nabeul, Tunisie, 4-7 juin 2007. Cirad, Montpellier (France).
- Douaoui, A.E.K., Yahiaoui, I. (2015), *Combination of remote sensing and kriging to improve soil salinity mapping in the Hmadna plain (Algeria)*. Soil-Water Journal, Special Issue: **1–5**.
- Doumit, J. A., Sakr, S. C. (2015), *La cartographie du sol nu dans la vallée de la Bekaa à partir de la télédétection*. Proceedings of the International Conference "InterCarto. InterGIS", **21**, pp. 19–24.
- El Bouhissi, M., Bachir Bouiadjra, S. E., Fertout-Mouri, N., Benabdeli, K. (2022), *Etude diachronique de la dynamique du couvert végétal des forêts domaniales de la région de Merine (Algérie occidentale)*. Geo-Eco-Trop, **46**(1), pp. 125–136.
- Farah A. K. (2014), *Changement climatique ou variabilité climatique dans l'Est algérien*. Thèse de magister, Université Constantine 1, 109 p.
- FAO (1995), *L'irrigation en Afrique en chiffres*, FAO Rapports sur l'eau, (7), 336 p.
- FAO (2005), *L'irrigation en Afrique en chiffres Enquête AQUASTAT*. Division de la mise en valeur des terres et des eaux, Rome, FAO Rapport sur l'eau (29), 637 p.
- FAO (2010), *Guidelines on spate irrigation*, FAO Irrigation and Drainage Paper, (65), 233 p. Rome.
- FAO (2015a), *AQUASTAT Profil de Pays – Algérie*, 18 p.
- FAO (2015b), *AQUASTAT Profil de Pays – Maroc*, 18 p.
- Freni, G., Liuzzo, L. (2019), *Effectiveness of rainwater harvesting systems for flood reduction in residential urban areas*. Water, **11**(7), 1389.
- Gaagai, A., Aouissi, H. A., Maalem, S. E., Ababsa, M. (2020), *Impact of climate change and anthropic activity on the water quality of Babar Dam in Algeria*. Global Journal of Engineering Sciences, **6**(4).
- Gallego, F. J., Kussul, N., Skakun, S., Kravchenko, O., Shelestov, A., Kussul, O. (2014), *Efficiency assessment of using satellite data for crop area estimation in Ukraine*. International Journal of Applied Earth Observation and Geoinformation, **29**, pp. 22–30.
- Gao, B.-C. (1996), *NDWI—A normalized difference water index for remote sensing of vegetation liquid water from space*. Remote Sensing of Environment, **58**(3), pp. 257–266.
- Ghebreamlak, A. Z., Tanakamaru, H., Tada, A., Ahmed Adam, B. M., Elamin, K. A. (2018), *Satellite-based mapping of cultivated area in Gash Delta Spate irrigation system, Sudan*. Remote Sensing, **10**(2), 186.
- Guidoum, A. (2017), *Caractérisation hydrologique et analyse du transport solide en suspension dans trois ensembles hydrographiques du Nord-Est algérien. Etude de cas dans la Seybouse, les hautes plaines constantinoises et Chott Melghir (Coupe Nord-Sud)*. Thèse de doctorat, Université Mohamed Khider de Biskra, 349 p.
- Gulácsi, A., Kovács, F. (2015), *Drought monitoring with spectral indices calculated from MODIS satellite images in Hungary*. Journal of Environmental Geography, **8**(3-4), pp. 11–20.
- Gumma, M. K., Thenkabail, P. S., Hideto, F., Nelson, A., Dheeravath, V., Busia, D., Rala, A. (2011), *Mapping irrigated areas of Ghana using fusion of 30 m and 250 m resolution remote-sensing data*. Remote Sensing, **3**(4), pp. 816–835.
- Gu, Y., Hunt, E., Wardlow, B., Basara, J. B., Brown, J. F., Verdin, J. P. (2008), *Evaluation of MODIS NDVI and NDWI for vegetation drought monitoring using Oklahoma Mesonet soil moisture data*. Geophysical Research Letters, **35**(22): L22401.
- Hauouari, M., Azaiez, M. N. (2001), *Optimal cropping patterns under water deficits*. European Journal of Operational Research, **130**(1), pp. 133–146.
- Hearn, K. P., Álvarez-Mozos, J. (2021), *A diachronic analysis of a changing landscape on the Duero river borderlands of Spain and Portugal combining remote sensing and ethnographic approaches*. Sustainability, **13**(24), 13962.

- IPTRID – Programme International pour la Technologie et la Recherche en Irrigation et Drainage (2006), *Conférence électronique sur la salinisation: Extension de la salinisation et stratégies de prévention et réhabilitation*. Du 6 février au 6 mars 2006. 12 p.
- Khadraoui, A. Taleb S. (2008), *Qualité des eaux dans le Sud algérien : potabilité – pollution et impact sur le milieu*. Éditions Khyam, Constantine, 367 p.
- Khan, N. M., Rastoskuev, V. V., Shalina, E. V., Sato, Y. (2001), *Mapping salt-affected soils using remote sensing indicators - a simple approach with the use of GIS IDRISI*. In 22nd Asian Conference on Remote Sensing. 5 - 9 November 2001, Singapore.
- Khan, N. M., Rastoskuev, V. V., Sato, Y., Shiozawa, S. (2005), *Assessment of hydrosaline land degradation by using a simple approach of remote sensing indicators*. Agricultural Water Management, **77**(1-3), pp. 96–109.
- Koull, N., Helimi, S., Mihoub, A., Mokhtari, S., Kherraze, M. E., Aouissi, H. A. (2022), *Integración de SIG y análisis jerárquico multi-criterio para analizar la idoneidad de la tierra para los cereales en la zona árida de Argelia*. International Journal of Agriculture and Natural Resources, **49**(1), pp. 36–50.
- Lamhamedi, B. E., Jnah, N., Sebari, I., Benbahria, Z. (2017), *Extraction automatique des zones irriguées dans la région du Gharb par analyse d'image basée-objets des images Landsat 8*. Revue Marocaine des Sciences Agronomiques et Vétérinaires, **5**(2), pp. 170–177.
- Legros, J. P. (2009), *La salinisation des terres dans le monde*. Académie des Sciences et Lettres de Montpellier, conférence n°4069, Bull. n°40, pp. 257–269.
- Lillesand, T. M., Kiefer, R. W. (1994), *Remote Sensing and Image Interpretation*. USA: John Wiley & Sons. 750 p.
- Liou, Y.-A., Kar, S. K. (2014), *Evapotranspiration estimation with remote sensing and various surface energy balance algorithms—A review*. Energies, **7**(5), pp. 2821–2849.
- Lobell, D. B. (2013), *The use of satellite data for crop yield gap analysis*. Field Crops Research, **143**, pp. 56–64.
- Loi, D. T., Chou, T. Y., Fang, Y. M. (2017), *Integration of GIS and remote sensing for evaluating forest canopy density index in Thai Nguyen Province, Vietnam*. International Journal of Environmental Science and Development, **8**(8), pp. 539–542.
- Mebarki, A. (2005), *Hydrologie des bassins de l'Est algérien : ressources en eau, aménagement et environnement*. Université Frères Mentouri de Constantine. Thèse de doctorat d'État, 360 p.
- Metternicht, G. I., Zinck, J. A. (2003), *Remote sensing of soil salinity: potentials and constraints*. Remote sensing of Environment, **85**(1), pp. 1–20.
- Mondal, S., Jeganathan, C., Sinha, N. K., Rajan, H., Roy, T., Kumar, P. (2014), *Extracting seasonal cropping patterns using multi-temporal vegetation indices from IRS LISS-III data in Muzaffarpur District of Bihar, India*. The Egyptian Journal of Remote Sensing and Space Science, **17**(2), pp. 123–134.
- Pervez, M. S., Brown, J. F. (2010), *Mapping irrigated lands at 250-m scale by merging MODIS data and national agricultural statistics*. Remote Sensing, **2**(10), pp. 2388–2412.
- Pervez, M. S., Budde, M., Rowland, J. (2014), *Mapping irrigated areas in Afghanistan over the past decade using MODIS NDVI*. Remote Sensing of Environment, **149**, pp. 155–165.
- Rikimaru, A., Roy, P. S., Miyatake, S. (2002), *Tropical forest cover density mapping*. Tropical Ecology, **43**(1), pp. 39–47.
- Rondeaux, G., Steven, M., Baret, F. (1996), *Optimization of soil-adjusted vegetation indices*. Remote Sensing of Environment, **55**(2), pp. 95–107.
- Rouse, J. W., Haas, R. H., Schell, J. A., Deering, D. W. (1974), *Monitoring vegetation systems in the Great Plains with ERTS, in Third earth resources technology satellite – 1 symposium*. vol. 1: technical presentations, Section A, (coord. Stanley C. Freden, Enrico P. Mercanti & Margaret A. Becker). NASA Washington, D.C.: SP-351: pp. 309–317.
- Sahbeni, G., Ngabire, M., Musyimi, P. K., Székely, B. (2023), *Challenges and opportunities in remote sensing for soil salinization mapping and monitoring: A review*. Remote Sensing, **15**(10), 2540.
- Salmon, J. M., Friedl, M. A., Frohling, S., Wisser, D., Douglas, E. M. (2015), *Global rain-fed, irrigated, and paddy croplands: A new high resolution map derived from remote sensing, crop inventories and climate data*. International Journal of Applied Earth Observation and Geoinformation, **38**, pp. 321–334.
- Sahbajjal, E., Dashtekian, K. (2013), *Analysis of land use-land covers changes using normalized difference vegetation index (NDVI) differencing and classification methods*. African Journal of Agricultural Research, **8**(37), pp. 4614–4622.
- Schmedtmann, J., Campagnolo, M. L. (2015), *Reliable crop identification with satellite imagery in the context of common agriculture policy subsidy control*. Remote Sensing, **7**(7), pp. 9325–9346.
- Schmid, T., Koch, M., Gumuzzio, J. (2008), *Applications of hyperspectral imagery to soil salinity mapping*, in *Remote sensing of soil salinization: impact on land manage*, (coord. Metternicht, G., & Zinck, A.), Edit. CRC Press, Boca Raton London New York, pp. 113–139.
- Serrano, J., Shahidian, S., Marques Da Silva, J. (2019), *Evaluation of normalized difference water index as a tool for monitoring pasture seasonal and inter-annual variability in a Mediterranean agro-silvo-pastoral system*. Water, **11**(1), 62.
- Singh, R. K., Liu, S., Tieszen, L. L., Suyker, A. E., Verma, S. B. (2012), *Estimating seasonal evapotranspiration from temporal satellite images*. Irrigation Science, **30**(4), pp. 303–313.
- Singh, R. P., Sirohi, A. (1994), *Spectral reflectance properties of different types of soil surfaces*. ISPRS Journal of Photogrammetry and Remote Sensing, **49**(4), pp. 34–40.

- Soomro, A. G., Babar, M. M., Arshad, M., Memon, A., Naeem, B., Ashraf, A. (2020), *Spatiotemporal variability in spate irrigation systems in Khirthar National Range, Sindh, Pakistan (case study)*, *Acta Geophysica*, **68**, pp. 219–228.
- Sultan, B., Djellouli, Y. (2013), *Sécheresse et canicule : incidence et prise en compte*, in *Le développement durable à découvert* (coord. Euzen, A., Eymard, L., & Gaill, F.), Edit. CNRS Éditions, Paris, pp. 218–219.
- Tebbi, F. Z. (2014), *Modélisation de la régularisation des barrages dans la région des Aurès*. Thèse de doctorat, Université Hadj Lakhdar de Batna, 123 p.
- Thibaut, K., Ozer, P. (2021), *Les sécheresses en Wallonie, un nouveau défi du changement climatique ? Quelques pistes pour améliorer la gestion de ce phénomène*. *Geo-Eco-Trop*, **45**(3), pp. 517–527.
- Thirukanthan, C. S., Azra, M. N., Abu Seman, N. J., Agos, S. M., Arifin, H., Aouissi, H. A., Lananan, F., Gao, H. (2023), *A scientometric review of climate change and research on crabs*, *Journal of Sea Research*, **193**: 102386.
- Tucker, C. J. (1979), *Red and photographic infrared linear combinations for monitoring vegetation*. *Remote Sensing of Environment*, **8**(2), pp. 127–150.
- van Halsema, G. E., Vincent, L. (2012), *Efficiency and productivity terms for water management: A matter of contextual relativism versus general absolutism*. *Agricultural Water Management*, **108**, pp. 9–15.
- Wgmn, J., Vmi. C. (2020), *Investigate the sensitivity of the satellite-based agricultural drought indices to monitor the drought condition of paddy and introduction to enhanced multi-temporal drought indices*. *Journal of Remote Sensing and GIS*, **9**: 272.
- Zuhriddin, J., Young-Jin, A. (2023), *Sustainable water management and elimination of water scarcity: a case study in a remote district of Uzbekistan*, *Revue Roumaine de Géographie / Romanian Journal of Geography*, **67**(2), pp. 151–162.

Received July 26, 2024

